Capturing the Local Adsorption Structures of Carbon Dioxide in Polyamine-Impregnated Mesoporous Silica Adsorbents

Shing-Jong Huang,*,[†] Chin-Te Hung,[§] Anmin Zheng,[‖] Jen-Shan Lin,[§,⊥] Chun-Fei Yang,[§,⊥] Yu-Chi Chang,[⊥] Feng Deng,[‖] and Shang-Bin Liu*,[§,‡]

[†]Instrumentation Center, National Taiwan University, 1, Sec. 4, Roosevelt Road, Taipei 10617, Taiwan

[§]Institute of Atomic and Molecular Sciences, Academia Sinica, 1, Sec. 4, Roosevelt Road, Taipei 10617, Taiwan

[‖]State Key Laboratory of Magnetic Resonance and Atomic and Molecular Physics, Wuhan Center for Magnetic Resonance, Wuhan Institute of Physics and Mathematics, Chinese Academy of Sciences, West No. 30 Xiao Hong Shan, Wuhan 430071, China

[⊥]Department of Chemical and Materials Engineering, Tamkang University, 151, Yingzhuan Road, New Taipei City 25137, Taiwan

[‡]Department of Chemistry, National Taiwan Normal University, 88, Sec. 4, Ting-Chow Road, Taipei 11677, Taiwan

S *Supporting Information*

ABSTRACT: Interactions between amines and carbon dioxide (CO_2) are essential to amine-functionalized solid adsorbents for carbon capture, and an in-depth knowledge of these interactions is crucial to adsorbent design and fabrication as well as adsorption/desorption processes. The local structures of CO_2 adsorbed on a tetraethylenepentamine-impregnated mesoporous silica SBA-15 were investigated by solid-state $^{13}C\{^{14}N\}$ S-RESPDOR MAS NMR technique and theoretical DFT calculations. Two types of adsorption species, namely, secondary and tertiary carbamates as well as distant ammonium groups were identified together with their relative concentrations and relevant ^{14}N quadrupolar parameters. Moreover, a dipolar coupling of 716 Hz was derived, corresponding to a $^{13}C-^{14}N$ internuclear distance of 1.45 Å. These experimental data are in excellent agreement with results obtained from DFT calculations, revealing that the distribution of surface primary and secondary amines readily dictates the CO_2 adsorption/desorption properties of the adsorbent.

SECTION: Surfaces, Interfaces, Porous Materials, and Catalysis
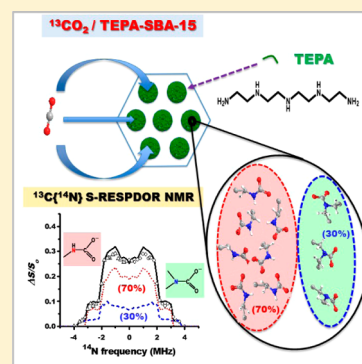
In view of the increasing demands in CO_2 capture and sequestration/utilization (CCS/CCU) technologies,[1−3] fabrication and implementation of novel CO_2 adsorbents with desirable sorption/desorption properties, durability, and cost-effective regeneration schemes have drawn considerable R&D attention.[4,5] Many existing commercial processes utilize alkanolamines as adsorbents;[6,7] however, those gas−liquid adsorption schemes are handicapped by fated issues such as low CO_2 uptake capacity, high equipment corrosion rate, high absorbent makeup rate, and high energy consumption. In this context, gas−solid adsorption schemes exploiting solid adsorbents, such as zeolites,[8−11] carbons,[12,13] organic polymers,[14,15] metal organic frameworks,[16−18] ordered mesoporous silicas (OMSs)[19−24] and so on, are believed to be a preferable alternative. Among them, extensive studies have been made on amine-modified OMSs[19−33] owing to their superior CO_2 adsorption capacity and durability. Nonetheless, despite plenteous spectroscopic studies on these adsorption systems by infrared (IR)[30−37] and solid-state ^{13}C cross-polarization magic-angle-spinning (CP-MAS) NMR[38,39] techniques, relevant reports emphasized mostly on the identification of chemisorbed species rather than the local structures of the adsorbed CO_2. For example, ^{13}C CP-MAS NMR of CO_2 adsorbed on amine-modified nanoporous materials has been used to identify the formation of carbamate and carbamic acid[38] as well as the formation of urea species due to CO_2-induced degradation.[39] In terms of amine-modified OMS systems, information on interactions between CO_2 adsorbate and amine moieties residing on the surfaces of the mesoporous adsorbent and relevant adsorption structures at the atomic level are essential for understanding detailed CO_2 uptake and release phenomena. Relevant information is crucial for innovative design and fabrication of prospective adsorbents as well as implementation of the adsorption/desorption processes.[40−49]

Solid-state NMR (SSNMR) has becoming a powerful tool not only for characterization of local structure but also site-specific quantitative analysis. Made available by the grafted amine functional groups, there are two nuclear spin isotopes for nitrogen, namely ^{14}N ($I = 1$) and ^{15}N ($I = 1/2$). While ^{15}N is commonly employed in NMR investigations involving N atoms owing to simplicity of spectra facilitated by the spin 1/2 nucleus, it has a much lower natural abundance (0.36%) compared with ^{14}N (99.64%). To avoid costly preparation of

isotope-enriched samples, we have chosen to focus on study of ^{14}N, which is a quadrupolar nucleus with a relatively lower nuclear gyromagnetic ratio (γ).

A specific amine-impregnated mesoporous silica SBA-15 sample loaded with 50 wt % tetraethylenepentamine (TEPA) was prepared[24] (see the Supporting Information; hereafter denoted as SI) and exploited as adsorbent in the present study. This reference adsorbent (hereafter denoted as TEPA-SBA-15) was found to exhibit anticipated textural properties (Figure S1; SI) and a CO_2 uptake capacity as high as 3.3 mmol per gram adsorbent (Figure S2; SI). To afford adequate ^{13}C NMR signal of the chemisorbed CO_2 species, we used isotope-enriched $^{13}CO_2$ to prepare $^{13}CO_2$-loaded TEPA-SBA-15 sample (see SI). The ^{13}C CP-MAS NMR spectrum (Figure S3; SI) showed a singlet peak at ca. 164.2 ppm, which may be attributed to the presence of carbamate ($NCOO^-$) species.[38,39] Likewise, the ^{15}N CP-MAS NMR spectrum (Figure S4; SI) revealed two resonance peaks at −298.0 and −350.7 ppm, which may be assigned to carbamate species and amine/ammonium groups, respectively.[38] These spectra indicate that the carbamate species form on the amine groups upon CO_2 adsorption, as illustrated in Scheme 1.

Scheme 1. Possible Local Structures of CO₂ Adsorbed on Amine Functional Groups
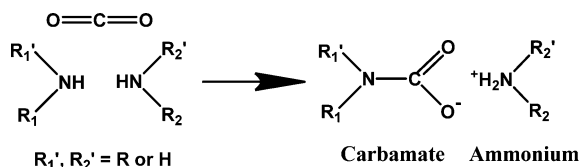
To further explore interactions between CO_2 and amine moieties, we employed the $^{13}C\{^{14}N\}$ symmetry-based rotational-echo saturation-pulse double-resonance (S-RESPDOR) MAS NMR technique[50−52] on $^{13}CO_2$-loaded TEPA-SBA-15 sample. A schematic layout of this multinuclear dipolar recoupling pulse sequence is shown in Figure S5a (SI). Here an improved S-RESPDOR technique was adopted for the determination of $^{13}C-^{14}N$ internuclear distance instead of the conventional rotational echo adiabatic passage double resonance (REAPDOR) method[53] mainly due to less rigorous requirement on radio frequency (RF) field strength for the ^{14}N channel. Additional advantage of S-RESPDOR over R-RESPDOR[51] is that the signal fraction, $\Delta S/S_o = (S_o - S)/S_o$, is independent of the relative orientation of the internuclear vector with respect to chemical shift anisotropy (CSA) and quadrupolar interactions.[52] In addition, Gan[50] introduced a novel method for measuring nitrogen quadrupolar coupling using ^{13}C-detected ^{14}N wide-line NMR, by which the first-order ^{14}N spectra may readily be obtained through the ^{13}C signal fraction profile of RESPDOR while sweeping the frequency of the ^{14}N saturation pulse.

It is noteworthy that the signal fraction ($\Delta S/S_o$) of the dipolar dephasing curve acquired by the $^{13}C\{^{14}N\}$ S-RESPDOR NMR sequence (Figure S5a; SI) for the carbamate species depends on its motional dynamics. As illustrated in Figure S6 (see SI), the signal fraction tends to increase gradually with decreasing temperature and eventually reaches a plateau at ca. 232 K regardless of the duration of dipolar recoupling (τ) used. This indicates that the molecular motions associated with CO_2 adsorption/desorption dynamics should be effectively frozen at

temperatures below ca. 230 K. Thus, further experiments were carried out at 226 K to avoid complications due to motional averaging. Moreover, it is anticipated that quadrupolar couplings associated with the ^{14}N nucleus should be sensitive to the local structures of the grafted amines while in the presence of CO_2 adsorbate, rendering detection of site-specific information. Thus, the ^{13}C-detected ^{14}N wide-line NMR technique[50] was adopted to acquire the first-order ^{14}N quadrupolar spectra through the S-RESPDOR sequence under ^{14}N frequency sweeping. It is noteworthy that the ^{14}N Larmor frequency was set identical to isotropic chemical shift of the carbamate resonance while acquiring the quadrupolar spectra.

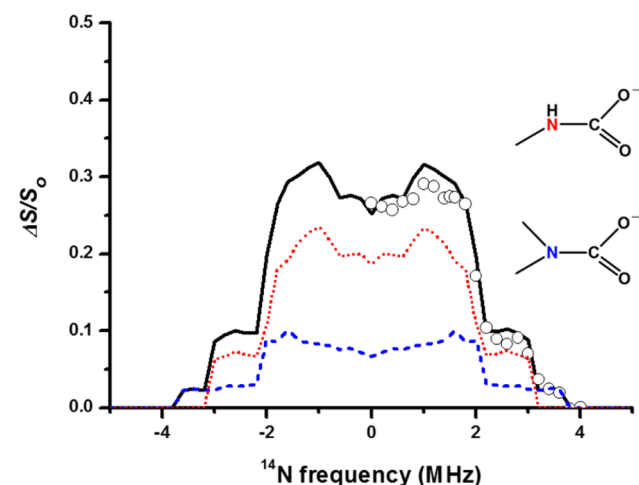Figures 1 and 2 display the spectrum recorded with a dephasing time (τ) of 3.20 and 11.52 ms, respectively. The

Figure 1. ^{13}C-detected ^{14}N wide-line NMR spectrum of $^{13}CO_2$ adsorbed on TEPA-SBA-15 recorded by the S-RESPDOR NMR sequence with a dephasing time of τ = 3.2 ms (open circles). The dotted and dashed curves are simulated spectra associated with secondary and tertiary carbamate species with a relative contribution of 70 and 30%, respectively. The solid curve represents the sum of the two simulated spectra.
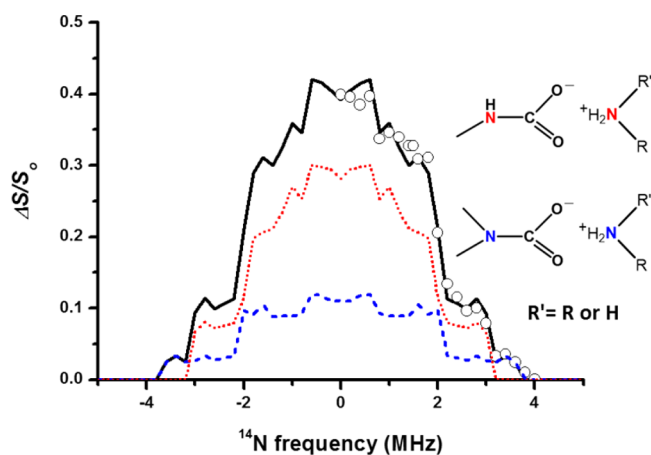

Figure 2. First-order ^{14}N quadrupolar spectra similar to Figure 1 but acquired with τ = 11.52 ms. The dotted and dashed curves are simulated spectra associated with secondary and tertiary carbamate–ammonium ion pairs with a relative fraction of 70 and 30%, respectively. The solid curve represents the sum of the two simulated spectra.

profile of wide-line spectra was recorded by sweeping the ^{14}N resonance frequency from 0 to 4 MHz with a step interval of 0.2 MHz. However, limited by the tuning range of the probehead available in our facility, the data points in the low-frequency region (from 0 to −4 MHz) were undetectable; nonetheless, they can readily be derived from the mirror reflections of the high-frequency results.[50] It is noteworthy that the quadrupolar lineshapes so observed exhibit the characteristics of multiplet pattern. In particular, two distinct edges at ca. 3.1 and 3.7 MHz may be identified in the spectrum recorded with dephasing time τ = 3.2 ms (Figure 1), indicating the existence of two nitrogen sites. Further spectral simulations based on a two-spin model assuming a ^{13}C−^{14}N internuclear distance of 1.45 Å revealed that the two CO_2 adsorption sites corresponding to the two carbamate species having ^{14}N quadrupolar coupling constants (C_Q) of 4.1 and 4.9 MHz and asymmetric factors (η) of 0.30 and 0.15 have contributions of ca. 70 and 30%, respectively. The relative contributions may be quantitatively estimated owing to the fact that they remain unchanged even in the presence of ^{13}C−^{13}C spin diffusion (Figures S7 and S5b; SI). At such short dephasing time (3.2 ms), signal contributions predominantly arising from proximate ^{13}C−^{14}N couplings may be anticipated. Thus, the former trace may be ascribed due to spin system associated with secondary carbamate species, whereas the latter is due to tertiary carbamates. These results are in good agreement with data obtained from theoretical DFT calculations (see SI), as depicted in Table 1.

Table 1. Comparisons of Experimental and Theoretical ^{14}N Quadrupolar Parameters for Assorted Carbamate and Ammonium Groups

	C_Q (MHz)		η	
species	exptl	calcd	exptl	calcd
secondary carbamate	4.1	4.39	0.30	0.19
tertiary carbamate	4.9	5.06	0.15	0.15
primary ammonium	1.5	1.07	0.20	0.24
secondary ammonium	1.5	0.88	0.20	0.26

As the dephasing time was prolonged to 11.52 ms, contributions from coupling of ^{13}C with distant nitrogen sites were also observed, leading to additional features in the multiplet pattern, especially within the range of −1.0 and 1.0 MHz (Figure 2). To facilitate spectral simulation, an additional ^{14}N quadrupolar coupling with C_Q = 1.5 MHz and η = 0.20 was introduced by assuming a ^{13}C−^{14}N internuclear distance of 3.10 Å. As shown in Table 1, the C_Q value so estimated is somewhat greater than the predicted values for primary (1.07 MHz) and secondary (0.88 MHz) ammonium groups based on a ^{14}N−^{13}C−^{14}N three-spin model. Unfortunately, limited by spectral resolution and possible experimental error, more accurate analysis for quadrupolar parameters of such remote coupling may not be attained.

In general, detailed information on dipolar couplings may not be extracted easily from the complicated S-RESPDOR dephasing curves of the sophisticated three-spin system. In the presence case, however, because a moderate C_Q value (1.5 MHz) was derived from ammonium ^{14}N, the dipolar recoupling associated with the ammonium group could be effectively depressed by offsetting the frequency of the ^{14}N saturation pulse large enough to avoid altering the ^{14}N spin states of

ammonium groups. In this context, the signal fraction curve so obtained can be regarded as contributions from a two-spin system, facilitating a more accurate determination of the ^{13}C−^{14}N internuclear distance in carbamate species. As such, a fixed ^{14}N irradiation frequency offset at 1.8 MHz with respect to the isotropic chemical shift of carbamate was chosen to alter the ^{14}N spin states of ammonium groups as negligibly as possible and, meanwhile, to preserve significant signal fractions, which is essential for the determination of internuclear distance. Figure 3 displays the S-RESPDOR dipolar dephasing curve
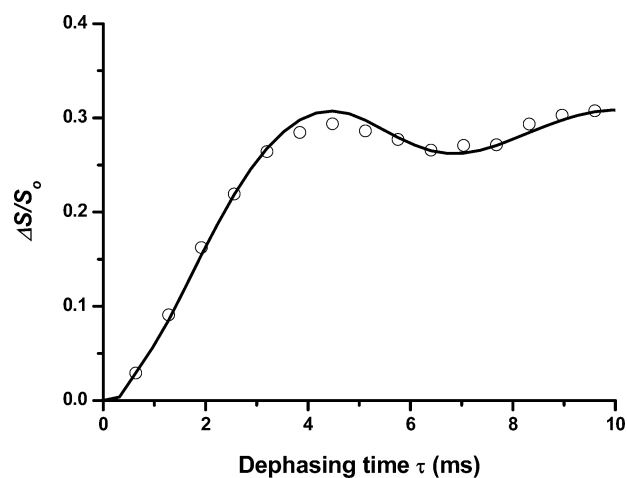

Figure 3. Variations of signal fraction with dipolar dephasing time for $^{13}CO_2$ adsorbed on TEPA-SBA-15 recorded by the ^{13}C{^{14}N} S-RESPDOR sequence at a fixed ^{14}N frequency of 1.8 MHz with respect to the isotropic chemical shift of carbamate. The solid curve represents simulated result.

acquired with a fixed ^{14}N irradiation frequency offset at 1.8 MHz with respect to the isotropic chemical shift of carbamate. Accordingly, a dipolar coupling of 716 Hz, which corresponds to a ^{13}C−^{14}N distance of 1.45 Å, was derived. The experimental bond distance so obtained is in excellent agreement with that of carbamate (1.46 Å) rather than carbamic (1.35 Å) species predicted by theoretical DFT calculations (Figure S8; SI).

In view of the fact that there are two primary and three secondary amines in each TEPA molecule, the results obtained herein therefore reveal that primary amines are the preferential CO_2 adsorption sites and that secondary carbamate species are thermodynamically more stable than their tertiary counterparts. These results are consistent with available adsorption data obtained from primary and secondary amine-grafted mesoporous silica.[27,28] To the best of our knowledge, this is the first direct simultaneous determination of CO_2 adsorption features on both primary and secondary amine groups tethered on the same adsorbent ligand.

In summary, we have demonstrated that solid-state ^{13}C{^{14}N} S-RESPDOR MAS NMR is a useful technique for probing the detailed adsorption structure of $^{13}CO_2$ on amine-impregnated solid adsorbents. Taking advantages of the ^{14}N quadrupolar parameters, which are sensitive to the local structures of the adsorption state, preferred CO_2 adsorption sites and their relevant populations over different carbamate species may be determined. Accordingly, the adsorption/desorption features of polyamine-impregnated adsorbents may readily be modulated by controlling the amounts of primary and secondary amine groups on the polyamine. Moreover, while the presence of

primary amines is preferred for enhancement in CO_2 uptake capacity,[27] secondary amines are more favorable in terms of lower energy consumption during regeneration.

■ ASSOCIATED CONTENT

Ⓢ Supporting Information

Details of sample preparation, SSNMR experiments, spectral simulations, DFT calculations, and assorted experiment results including adsorption kinetic data, SSNMR spectra, and optimized adsorption structures. This material is available free of charge via the Internet at http://pubs.acs.org.

■ AUTHOR INFORMATION

Corresponding Authors
*E-mail: shingjonghuang@ntu.edu.tw (S.-J.H.).
*E-mail: sbliu@sinica.edu.tw (S.-B.L.).

Notes
The authors declare no competing financial interest.

■ ACKNOWLEDGMENTS

■ REFERENCES

(1) *The Global Status of CCS: 2103*; Global CCS Institute: Melbourne, Australia, 2013.

(2) Working Group III of the Intergovernmental Panel on Climate Change. In *IPCC Special Report on Carbon Dioxide Capture and Storage*; Metz, B., Davidson, O., de Coninck, H. C., Loos, M., Meyer, L. A., Eds.; Cambridge University Press: Cambridge, U.K., 2005.

(3) Strying, P.; Jansen, D.; de Coninck, H.; Reith, H.; Armstrong, K. *Carbon Capture and Utilisation in the Green Economy: Using CO2 to Manufacture Fuel, Chemicals and Materials*; The Centre for Low Carbon Futures: York, U.K., 2011; Report Number 501.

(4) Morris, R. E.; Wheatley, P. S. Gas Storage in Nanoporous Materials. *Angew. Chem., Int. Ed.* 2008, 47, 4966−4981.

(5) Markewitz, P.; Kuckshinrichs, W.; Leitner, W.; Linssen, J.; Zapp, P.; Bongartz, R.; Schreiber, A.; Muller, T. E. Worldwide Innovations in the Development of Carbon Capture Technologies and the Utilization of CO_2. *Energy Environ. Sci.* 2012, 5, 7281−7305.

(6) Rinker, E. B.; Ashour, S. S.; Sandall, O. C. Absorption of Carbon Dioxide into Aqueous Blends of Diethanolamine and Methyldiethanolamine. *Ind. Eng. Chem. Res.* 2000, 39, 4346−4356.

(7) Patil, G. N.; Vaidya, P. D.; Kenig, E. Y. Reaction Kinetics of CO_2 in Aqueous Methyl- and Dimethyl-Monoethanolamine Solutions. *Ind. Eng. Chem. Res.* 2011, 51, 1592−1600.

(8) Maurin, G.; Bell, R.; Kuchta, B.; Poyet, T.; Llewellyn, P. Adsorption of Non Polar and Quadrupolar Gases in Siliceous Faujasite: Molecular Simulations and Experiments. *Adsorption* 2005, 11, 331−336.

(9) Siriwardane, R. V.; Shen, M. S.; Fisher, E. P.; Losch, J. Adsorption of CO_2 on Zeolites at Moderate Temperatures. *Energy Fuels* 2005, 19, 1153−1159.

(10) Walton, K. S.; Abney, M. B.; LeVan, M. D. CO_2 Adsorption in Y and X Zeolites Modified by Alkali Metal Cation Exchange. *Microporous Mesoporous Mater.* 2006, 91, 78−84.

(11) Himeno, S.; Tomita, T.; Suzuki, K.; Yoshida, S. Characterization and Selectivity for Methane and Carbon Dioxide Adsorption on the All-Silica DD3R Zeolite. *Microporous Mesoporous Mater.* 2007, 98, 62−69.

(12) Himeno, S.; Komatsu, T.; Fujita, S. High-Pressure Adsorption Equilibria of Methane and Carbon Dioxide on Several Activated Carbons. *J. Chem. Eng. Data* 2005, 50, 369−376.

(13) Arenillas, A.; Smith, K. M.; Drage, T. C.; Snape, C. E. CO_2 Capture Using Some Fly Ash-Derived Carbon Materials. *Fuel* 2005, 84, 2204−2210.

(14) Navarro, J. A. R.; Barea, E.; Salas, J. M.; Masciocchi, N.; Galli, S.; Sironi, A.; Ania, C. O.; Parra, J. B. H_2, N_2, CO, and CO_2 Sorption Properties of a Series of Robust Sodalite-Type Microporous Coordination Polymers. *Inorg. Chem.* 2006, 45, 2397−2399.

(15) Thallapally, P. K.; McGrail, B. P.; Atwood, J. L.; Gaeta, C.; Tedesco, C.; Neri, P. Carbon Dioxide Capture in a Self-Assembled Organic Nanochannels. *Chem. Mater.* 2007, 19, 3355−3357.

(16) Millward, A. R.; Yaghi, O. M. Metal-Organic Frameworks with Exceptionally High Capacity for Storage of Carbon Dioxide at Room Temperature. *J. Am. Chem. Soc.* 2005, 127, 17998−17999.

(17) Ramsahye, N. A.; Maurin, G.; Bourrelly, S.; Llewellyn, P. L.; Loiseau, T.; Serre, C.; Férey, G. On the Breathing Effect of a Metal-Organic Framework upon CO_2 Adsorption: Monte Carlo Compared to Microcalorimetry Experiments. *Chem. Commun.* 2007, 3261−3263.

(18) Walton, K. S.; Millward, A. R.; Dubbeldam, D.; Frost, H.; Low, J. J.; Yaghi, O. M.; Snurr, R. Q. Understanding Inflections and Steps in Carbon Dioxide Adsorption Isotherms in Metal-Organic Frameworks. *J. Am. Chem. Soc.* 2008, 130, 406−407.

(19) Xu, X.; Song, C.; Andresen, J. M.; Miller, B. G.; Scaroni, A. W. Novel Polyethylenimine-Modified Mesoporous Molecular Sieve of MCM-41 Type as High-Capacity Adsorbent for CO_2 Capture. *Energy Fuels* 2002, 16, 1463−1469.

(20) Xu, X.; Song, C.; Miller, B. G.; Scaroni, A. W. Influence of Moisture on CO_2 Separation from Gas Mixture by a Nanoporous Adsorbent Based on Polyethylenimine-Modified Molecular Sieve MCM-41. *Ind. Eng. Chem. Res.* 2005, 44, 8113−8119.

(21) Kim, S.; Ida, J.; Guliants, V. V.; Lin, J. Y. S. Tailoring Pore Properties of MCM-48 Silica for Selective Adsorption of CO_2. *J. Phys. Chem. B* 2005, 109, 6287−6293.

(22) Harlick, P. J. E.; Sayari, A. Applications of Pore-Expanded Mesoporous Silica. 5. Triamine Grafted Material with Exceptional CO_2 Dynamic and Equilibrium Adsorption Performance. *Ind. Eng. Chem. Res.* 2007, 46, 446−458.

(23) Yue, M. B.; Chun, Y.; Cao, Y.; Dong, X.; Zhu, J. H. CO_2 Capture by As-Prepared SBA-15 with an Occluded Organic Template. *Adv. Funct. Mater.* 2006, 16, 1717−1722.

(24) Liu, S. H.; Wu, C. H.; Lee, H. K.; Liu, S. B. Highly Stable Amine-Modified Mesoporous Silica Materials for Efficient CO_2 Capture. *Top. Catal.* 2009, 53, 210−217.

(25) Choi, S.; Drese, J. H.; Jones, C. W. Adsorbent Materials for Carbon Dioxide Capture from Large Anthropogenic Point Sources. *ChemSusChem* 2009, 2, 796−854.

(26) Yu, C. H.; Huang, C. H.; Tan, C. S. A Review of CO_2 Capture by Absorption and Adsorption. *Aerosol Air Qual. Res.* 2012, 12, 745−769.

(27) Didas, S. A.; Kulkarni, A. R.; Sholl, D. S.; Jones, C. W. Role of Amine Structure on Carbon Dioxide Adsorption from Ultradilute Gas Streams such as Ambient Air. *ChemSusChem* 2012, 5, 2058−2064.

(28) Sayari, A.; Belmabkhout, Y.; Da'na, E. CO_2 Deactivation of Supported Amines: Does the Nature of Amine Matter? *Langmuir* 2012, 28, 4241−4247.

(29) Yan, X.; Zhang, L.; Zhang, Y.; Yang, G.; Yan, Z. Amine-Modified SBA-15: Effect of Pore Structure on the Performance for CO_2 Capture. *Ind. Eng. Chem. Res.* 2011, 50, 3220−3226.

(30) Chang, A. C. C.; Chuang, S. S. C.; Gray, M.; Soong, Y. In-Situ Infrared Study of CO_2 Adsorption on SBA-15 Grafted with γ-(Aminopropyl)triethoxysilane. *Energy Fuels* 2003, 17, 468−473.

(31) Khatri, R. A.; Chuang, S. S. C.; Soong, Y.; Gray, M. Carbon Dioxide Capture by Diamine-Grafted SBA-15: A Combined Fourier Transform Infrared and Mass Spectrometry Study. *Ind. Eng. Chem. Res.* 2005, 44, 3702−3708.

(32) Khatri, R. A.; Chuang, S. S. C.; Soong, Y.; Gray, M. Thermal and Chemical Stability of Regenerable Solid Amine Sorbent for CO_2 Capture. *Energy Fuels* 2006, 20, 1514−1520.

(33) Tanthana, J.; Chuang, S. S. C. In Situ Infrared Study of the Role of PEG in Stabilizing Silica-Supported Amines for CO_2 Capture. *ChemSusChem* **2010**, *3*, 957−964.

(34) Wang, X.; Schwartz, V.; Clark, J. C.; Ma, X.; Overbury, S. H.; Xu, X.; Song, C. Infrared Study of CO_2 Sorption over "Molecular Basket" Sorbent Consisting of Polyethylenimine-Modified Mesoporous Molecular Sieve. *J. Phys. Chem. C* **2009**, *113*, 7260−7268.

(35) Knöfel, C.; Martin, C.; Hornebecq, V.; Llewellyn, P. L. Study of Carbon Dioxide Adsorption on Mesoporous Aminopropylsilane-Functionalized Silica and Titania Combining Microcalorimetry and in Situ Infrared Spectroscopy. *J. Phys. Chem. C* **2009**, *113*, 21726−21734.

(36) Bacsik, Z.; Atluri, R.; Garcia-Bennett, A. E.; Hedin, N. Temperature-Induced Uptake of CO_2 and Formation of Carbamates in Mesocaged Silica Modified with *n*-Propylamines. *Langmuir* **2010**, *26*, 10013−10024.

(37) Danon, A.; Stair, P. C.; Weitz, E. FTIR Study of CO_2 Adsorption on Amine-Grafted SBA-15: Elucidation of Adsorbed Species. *J. Phys. Chem. C* **2011**, *115*, 11540−11549.

(38) Pinto, M. L.; Mafra, L.; Guil, J. M.; Pires, J.; Rocha, J. Adsorption and Activation of CO_2 by Amine-Modified Nanoporous Materials Studied by Solid-State NMR and $^{13}CO_2$ Adsorption. *Chem. Mater.* **2011**, *23*, 1387−1395.

(39) Sayari, A.; Heydari-Gorji, A.; Yang, Y. CO_2-Induced Degradation of Amine-Containing Adsorbents: Reaction Products and Pathways. *J. Am. Chem. Soc.* **2012**, *134*, 13834−13842.

(40) Barbarini, A.; Maggi, R.; Mazzacani, A.; Mori, G.; Sartori, G.; Sartorio, R. Cycloaddition of CO_2 to Epoxides over Both Homogeneous and Silica-Supported Guanidine Catalysts. *Tetrahedron Lett.* **2003**, *44*, 2931−2934.

(41) Srivastava, R.; Srinivas, D.; Ratnasamy, P. CO_2 Activation and Synthesis of Cyclic Carbonates and Alkyl/Aryl Carbamates over Adenine-Modified Ti-SBA-15 Solid Catalysts. *J. Catal.* **2005**, *233*, 1−15.

(42) Goettmann, F.; Thomas, A.; Antonietti, M. Metal-Free Activation of CO_2 by Mesoporous Graphitic Carbon Nitride. *Angew. Chem., Int. Ed.* **2007**, *46*, 2717−2720.

(43) Wong, W. L.; Chan, P. H.; Zhou, Z. Y.; Lee, K. H.; Cheung, K. C.; Wong, K. Y. A Robust Ionic Liquid as Reaction Medium and Efficient Organocatalyst for Carbon Dioxide Fixation. *ChemSusChem* **2008**, *1*, 67−70.

(44) Udayakumar, S.; Park, S. W.; Park, D. W.; Choi, B. S. Immobilization of Ionic Liquid on Hybrid MCM-41 System for the Chemical Fixation of Carbon Dioxide on Cyclic Carbonate. *Catal. Commun.* **2008**, *9*, 1563−1570.

(45) Prasetyanto, E. A.; Ansari, M. B.; Min, B. H.; Park, S. E. Melamine Tri-Silsesquioxane Bridged Periodic Mesoporous Organosilica as an Efficient Metal-Free Catalyst for CO_2 Activation. *Catal. Today* **2010**, *158*, 252−257.

(46) Lin, J.; Ding, Z.; Hou, Y.; Wang, X. Ionic Liquid Co-Catalyzed Artificial Photosynthesis of CO. *Sci. Rep.* **2013**, *3*, 1056.

(47) Planas, N.; Dzubak, A. L.; Poloni, R.; Lin, L. C.; McManus, A.; McDonald, T. M.; Neaton, J. B.; Long, J. R.; Smit, B.; Gagliardi, L. The Mechanism of Carbon Dioxide Adsorption in an Alkylamine-Functionalized Metal-Organic Framework. *J. Am. Chem. Soc.* **2013**, *135*, 7402−7405.

(48) Vaidhyanathan, R.; Iremonger, S. S.; Shimizu, G. K. H.; Boyd, P. G.; Alavi, S.; Woo, T. K. Direct Observation and Quantification of CO_2 Binding within an Amine-Functionalized Nanoporous Solid. *Science* **2010**, *330*, 650−653.

(49) Lastoskie, C. Caging Carbon Dioxide. *Science* **2010**, *330*, 595−596.

(50) Gan, Z. Measuring Nitrogen Quadrupolar Coupling with ^{13}C Detected Wide-Line ^{14}N NMR under Magic-Angle Spinning. *Chem. Commun.* **2008**, 868−870.

(51) Gan, Z. Measuring Multiple Carbon-Nitrogen Distances in Natural Abundant Solids using R-RESPDOR NMR. *Chem. Commun.* **2006**, 4712−4714.

(52) Chen, L.; Wang, Q.; Hu, B.; Lafon, O.; Trébosc, J.; Deng, F.; Amoureux, J. P. Measurement of Hetero-Nuclear Distances Using a Symmetry-Based Pulse Sequence in Solid-State NMR. *Phys. Chem. Chem. Phys.* **2010**, *12*, 9395−9405.

(53) Gullion, T. Measurement of Dipolar Interactions between Spin-1/2 and Quadrupolar Nuclei by Rotational-Echo, Adiabatic-Passage, Double-Resonance NMR. *Chem. Phys. Lett.* **1995**, *246*, 325−330.